17th Annual (International) Conference on Mechanical Engineering
May 19-21, 2009
75th Anniversary of University of Tehran
ISME 2009

# Soot Emission Prediction of a Turbo-charged DI Diesel Engine in Different Opening Ranges of Waste-gate Using Artificial Neural Network

M.Ghazikhani[1], I.Mirzaii[2]

[1]Assistant professor, Ferdowsi University of Mashhad; m_ ghazikhani@yahoo.com
[2]Ms. student, Ferdowsi University of Mashhad; imanmirzaii@gmail.com

**Abstract**

This study includes artificial neural network modeling (ANN) of a turbo-charged DI diesel engine. Six ranges of experimental data(conducted under the ECE-49, 13 mode standard test), were used for training the model. Inputs for ANN were inlet manifold pressure and temperature, mass flow rate of air, fuel consumption, torque and engine speed. Output was density of soot. Root mean squared-error, fraction of variance and mean absolute percentage error for predictions were found to be 3.4$\left(\frac{mg}{m^3}\right)$, 0.998 and 8.1% respectively.

**Keywords:** Artificial neural network, DI Diesel engines, waste-gated turbocharger, soot emission.

## Introduction

Diesel engines are able to operate at higher compression ratios than conventional gasoline engines and also they are lean burn. These reasons lead to better fuel economy than conventional gasoline engines. So they are widely used in transporting systems. Despite these advantages, diesel engines suffer from environmental drawbacks such as high level of exhaust $NO_x$, soot and particulate matter [1]. Because of harmful influence of these exhaust emissions on environment, there have been widespread attempts to reduce the exhaust emissions of diesel engines and consequently the influence of these emissions on environment.

For knowing the performance of the engine we can test the engine in every operation condition or we model it with artificial neural network (ANN) when sufficient test data is available for training and testing the accuracy of the engine. This approach was used to predict the performance and exhaust emissions of diesel engines [2, 6] and the effects of valve-timing in a spark ignition engine on the engine performance and fuel economy [7].

A neural network is a general mathematical computing paradigm that models the operations of biological neural systems. The nonlinear nature of neural networks, the ability of neural networks to learn from their environments in supervised as well as unsupervised ways, the universal approximation property of neural networks make them highly suited for solving complex problems[8].

## Experiments

The experiments were performed on a four cylinder, turbocharged DI diesel engine. The experiments in previous study [9] were repeated for four maximum inlet manifold pressures which were supplied by four opening ranges of waste-gate. In this study cause we need more data for training the ANN model we add three more maximum inlet manifold pressures. The additional maximum inlet manifold pressures are 0.15 bar, 0.2 bar and 0.35 bar.

## ANN MODEL

The ANN was trained and tested by means of the MATLAB software on a PC. The learning algorithm called back-propagation was applied for the feed-forward network. ANN model has one hidden layer which has 25 neurons. The inputs for the ANN are inlet manifold pressure, inlet manifold temperature, mass flow rate of inlet air, fuel consumption, torque and engine speed. The output is density of soot in the exhaust manifold. Levenberg–Marquardt (LM) algorithm has been used for the network. For training the neural network six ranges of pressures were used. Seventh range of pressure was kept for testing the accuracy of the trained network.

## Results and discussion

The ANN predictions for the density of soot emission of the DI diesel engine as a function of the experimental ones are shown in Fig. 1. The accuracy of the ANN predictions was evaluated with the help of a straight line indicating the perfect prediction. Also the comparison between actual values and predicted values are shown in Fig.2 and Fig.3. Because the range of soot density is from 2-200$\left(\frac{mg}{m^3}\right)$ we separated high density modes and low density modes in two different charts.

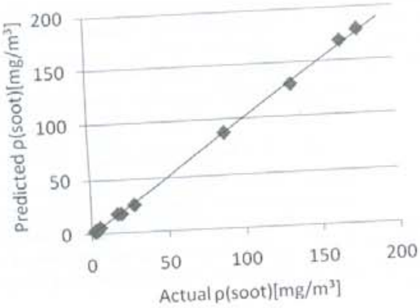


Fig.1. Comparison of actual and ANN approach values for density of soot emission

# Soot emission prediction of a turbo-charged DI diesel engine in different opening ranges of waste-gate using artificial neural network

**I.Mirzaii[1], M.Ghazikhani[2]**

[1]Ms. student, Ferdowsi University of Mashhad; imanmirzaii@gmail.com
[2]Assistant professor, Ferdowsi University of Mashhad; m_ ghazikhani@yahoo.com

## Abstract

This study is about soot emission prediction of a turbo-charged DI diesel engine in different opening ranges of waste-gate using artificial neural network. For training and testing the ANN model, different opening ranges of waste-gate were supplied using an adjustable spring to load the actuating rod of the waste-gate in which, increasing the opening range of the waste-gate decreases the inlet manifold pressure. The maximum inlet manifold pressures in test were 0.1 bar, 0.15 bar, 0.2 bar, 0.23 bar, 0.26 bar, 0.35 bar and 0.52 bar over atmosphere and experiments were conducted under the ECE-R49, 13 mode standard test. Using six ranges of the experimental data for training, an ANN model based on standard back-propagation algorithm for the engine was developed. Inputs for the ANN are inlet manifold pressure, inlet manifold temperature, mass flow rate of inlet air, fuel consumption, torque and engine speed. Output is density of soot in the exhaust manifold. The accuracy of the ANN was tested by comparing the predictions with seventh range of experimental results. Root mean squared-error (RMSE), fraction of variance ($R^2$) and mean absolute percentage error (MAPE) were found to be $3.4\left(\frac{mg}{m^3}\right)$, 0.998 and 8.1% respectively.

**Keywords:** Artificial neural network, DI Diesel engine, waste-gated turbocharger, soot emission.

## Introduction

Diesel engines are able to operate at higher compression ratios than conventional gasoline engines and also they are lean burn. These reasons lead to better fuel economy than conventional gasoline engines. So they are widely used in transporting systems. Despite these advantages, diesel engines suffer from environmental drawbacks such as high level of exhaust $NO_x$, soot and particulate matter [1]. Because of harmful influence of these exhaust emissions on environment, there have been widespread attempts to reduce the exhaust emissions of diesel engines and consequently the influence of these emissions on environment.

The inlet manifold air state has great effect on soot emission. Temperature has the greatest effect of any parameter on the sooting process by increasing all of the reaction rates involved in soot formation and oxidation [2]. High temperatures at the time of injection reduce air entrainment and increase the soot formation, while high temperatures at the end of the combustion enhance the burn-out of soot [2].

L.M. Pickett and D.L. Siebers [3], have studied a measurement of soot distributions in fuel jets injected into high-temperature, high-pressure diesel-like operating conditions were made in an optically accessible constant-volume combustion vessel. Their results show that peak soot level in a fuel jet increases with increasing ambient gas temperature, with the increase scaling linearly with temperature. Also they found, overall, the trends observed in diesel fuel jet soot closely correlate with the cross-sectional average equivalence ratio at the lift-off length, with soot levels decreasing as the equivalence ratio decreases [3]. So, for these reasons, any variation in the inlet manifold pressure which changes the in-cylinder gas temperature and pressure can affect the soot formation and soot oxidation in a diesel engine.

Artificial neural-network (ANN) models allow the modeling of physical phenomena in complex systems without requiring explicit mathematical representations. The use of ANNs for modeling the operation of internal combustion engines is a more recent progress. This approach was used to predict the performance and exhaust emissions of diesel engines [4-8] and the effects of valve-timing in a spark ignition engine on the engine performance and fuel economy [9]. Compressor's characteristic performance map was also investigated using ANNs [10].

In this study, the effects of opening range of waste gate (O.R.W.G.) on density of exhaust soot emission of a turbo-charged DI diesel engine is modeled by using an ANN. This approach was applied because testing the engine in our previous study [11] is a time consuming and expensive process. So we used ANN modeling as an alternative of the engine. In that study the maximum inlet manifold pressures which were supplied by changing the opening range of waste-gate were 0.1 bar, 0.23 bar, 0.26 bar and 0.52 bar over atmosphere and experiments were conducted under the ECE-R49, 13 mode standard test. Because we needed more data for modeling, we added three more ranges of inlet manifold pressures. The additional maximum inlet pressures are 0.15 bar, 0.2 bar and 0.35 bar.

## Experiments

As Fig. (1) shows, the experiments were performed on a four cylinder, turbocharged DI diesel engine. The main specifications of the diesel engine are given in table (1). The experiments in previous study were repeated for four maximum inlet manifold pressures which were supplied by four opening ranges of waste-gate under the ECE-R49, 13 mode standard test. In this study cause we needed more data for training the ANN model we added three more maximum inlet manifold pressures. The additional maximum inlet manifold pressures are 0.15 bar (W.G.O.R. No.5), 0.2 bar (W.G.O.R. No.6) and 0.35 bar (W.G.O.R. No.7). Torque was exerted to the engine by a Froude hydraulic dynamometer, and the engine speed was recorded using a magneto-electrical speed sensor. The temperature of inlet and exhaust manifold temperature were recorded utilizing K-type thermocouples while the pressure of inlet and exhaust manifold were measured using Bourdon pressure gage. The soot emission was measured using the AVL-415 soot analyzer. The measurements accuracies were listed in table (2). You can see schematic of the experimental setup in Fig. 1.

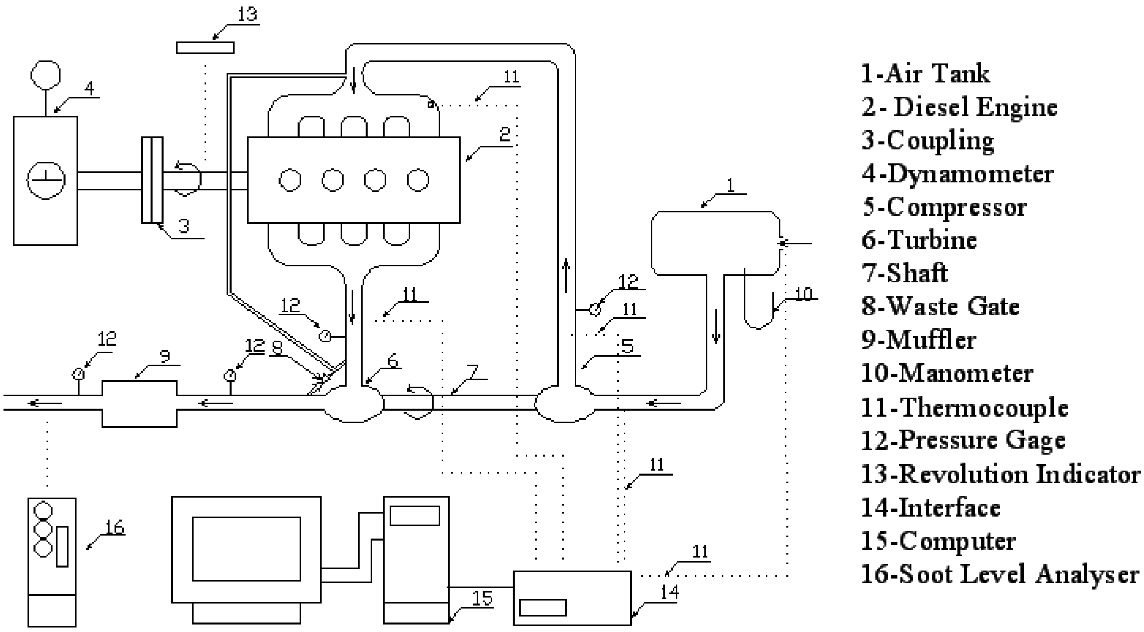


Fig.1. Schematic of the experimental setup

Table 1: OM314 engine specifications

| Engine and turbocharger | Specification |
|---|---|
| Engine type | 4 stroke diesel engine |
| Number of cylinder | 4 |
| Combustion chamber | Direct injection |
| Bore _ stroke (mm) | 97 × 128 |
| Piston displacement (cc) | 3784 |
| Compression ratio | 17:1 |
| Maximum power (hp) | 85 |
| Maximum torque (N.m) | 235 |
| Maximum speed (rpm) | 2800 |
| Turbocharger turbine | Radial type |
| Turbocharger compressor | Centrifugal type |

Table 2: Accuracies of the measurement

| Measurement | Accuracy |
|---|---|
| Torque | ±0.5 N.m |
| Speed | ±1 rpm |
| Soot | ±1 mg/m3 |
| Pressure | ±1 mm Hg |
| Temperature | ±0.1 _C |

**Brake specific soot calculation**

ECE-R49 test comprises the multi-mode steady state tests which each mode has a special load and speed with its special weighting factor [12]. At each mode, soot emission and engine power were recorded. Brake specific soot emission was calculated by equation (1) [12]:

$$S_{soot} = \sum_{1}^{13} \frac{\dot{m}_{soot}}{P_{b,s}} . W_f \qquad (1)$$

Where, corrected brake power is obtained using Equation (2):

$$P_{b,s} = \left(\frac{T.N.2\pi}{60 \times 1000}\right) . C_f \qquad (2)$$

According to page 270 of Ref. [10] $C_f$ is the correction factor which is given by Equation (3):

$$C_f = \frac{P_{s,d}}{P_m - P_{m,v}} \cdot \left(\frac{T_m}{T_s}\right)^{\frac{1}{2}} \tag{3}$$

The mass flow rate of soot is given by equation (4):

$$\dot{m}_{soot} = \rho_{soot} \cdot 10^{-3} \cdot Q_e \cdot 3600 \tag{4}$$

$\dot{Q}_e$ is the volumetric flow rate of exhaust gas and is obtained as follows:

$$\dot{Q}_e = \frac{\dot{m}_a + \dot{m}_f}{\rho_e} \tag{5}$$

The pressure of exhaust gas was measured by a pressure gage, so the exhaust gas density was obtained as:

$$\rho_e = \frac{p_e}{[0.287(T_e + 273)]} \tag{6}$$

Air mass flow rate is given by Equation (7):

$$\dot{m}_a = c_d \cdot A_o \cdot \sqrt{2 \times 9.81 \rho_l \cdot \Delta h_{orific} \cdot \rho_{air}} \tag{7}$$

Where $\Delta h_{orifice}$ is difference in elevation of orifice. Fuel mass flow rate is:

$$\dot{m}_f = \frac{50 \times 10^{-6}}{t_f} \rho_f \tag{8}$$

Where $\rho_f$ is diesel-fuel density which was equal to 830 kg/m$^3$ and $t_f$ is the required time for consumption of 50 cc of fuel.

Table 3: Waste gate opening range No. 5

| Mode No. | Torque (N.m) | Speed (rpm) | $T_c$ °C | $C_f$ | $P_{b,s}$ (kW) | Eq. ratio | $\dot{m}_{air}$ (kg/h) | $T_{exhaust}$ °C | $P_{exhaust}$ (Pa) | $\rho_{soot}$ (mg/m$^3$) | $S_{soot}$ (g/kWh) | $P_{inlet\ manifold}$ (bar) | $T_{inlet\ manifold}$ °C |
|---|---|---|---|---|---|---|---|---|---|---|---|---|---|
| 1 | 5 | 700 | 13 | 1.09 | 0.3996 | 0.15385 | 73.87 | 80 | 1415.4 | 3.3 | 0.05744 | 0.0162 | 24.5 |
| 2 | 23.5 | 1830 | 15 | 1.095 | 4.9315 | 0.23958 | 166.4 | 140 | 1423.0 | 2 | 0.00718 | 0.0477 | 29.4 |
| 3 | 58.5 | 1830 | 16 | 1.099 | 12.318 | 0.30002 | 173.6 | 170 | 1556.2 | 3.2 | 0.00515 | 0.0577 | 31 |
| 4 | 117.5 | 1830 | 17 | 1.1 | 24.775 | 0.43547 | 174.3 | 219 | 1665.0 | 5.2 | 0.00468 | 0.0792 | 32.2 |
| 5 | 176 | 1830 | 18 | 1.104 | 37.231 | 0.57230 | 175.4 | 283 | 1939.4 | 19.7 | 0.01351 | 0.101 | 33.8 |
| 6 | 235 | 1830 | 18 | 1.102 | 49.631 | 0.75028 | 168.8 | 362 | 2738.3 | 187.8 | 0.33259 | 0.132 | 36 |
| 7 | 5 | 700 | 17 | 1.099 | 0.4028 | 0.10310 | 83.9 | 190 | 1759.4 | 4.8 | 0.12251 | 0.02 | 29 |
| 8 | 194 | 2800 | 18 | 1.101 | 62.65 | 0.80510 | 226.6 | 415 | 5120.0 | 187.5 | 0.14985 | 0.15 | 40.5 |
| 9 | 145.5 | 2800 | 20 | 1.108 | 47.266 | 0.61932 | 231.1 | 363 | 4629.0 | 121.97 | 0.02420 | 0.122 | 39 |
| 10 | 97 | 2800 | 20 | 1.108 | 31.515 | 0.50218 | 227 | 302 | 4086.0 | 82 | 0.02159 | 0.111 | 37.0 |
| 11 | 48.5 | 2800 | 21 | 1.112 | 15.809 | 0.371470 | 226.4 | 241 | 3545.1 | 32 | 0.01495 | 0.0831 | 35.5 |
| 12 | 19.5 | 2800 | 22 | 1.113 | 6.3641 | 0.28682 | 229.7 | 205 | 3187.3 | 22.7 | 0.02482 | 0.0654 | 34.7 |
| 13 | 5 | 700 | 20 | 1.108 | 0.4061 | 0.125360 | 72.06 | 112 | 1687.3 | 3 | 0.05432 | 0.0124 | 24.8 |

Table 4: Waste gate opening range No. 6

| Mode No. | Torque (N.m) | Speed (rpm) | $T_c$ °C | $C_f$ | $P_{b,s}$ (kW) | Eq. ratio | $\dot{m}_{air}$ (kg/h) | $T_{exhaust}$ °C | $P_{exhaust}$ (Pa) | $\rho_{soot}$ (mg/m$^3$) | $S_{soot}$ (g/kWh) | $P_{inlet\ manifold}$ (bar) | $T_{inlet\ manifold}$ °C |
|---|---|---|---|---|---|---|---|---|---|---|---|---|---|
| 1 | 5 | 700 | 12 | 1.087 | 0.3985 | 0.16562 | 67.30 | 79 | 1399.4 | 3.4 | 0.05393 | 0.015 | 22.4 |
| 2 | 23.5 | 1830 | 15 | 1.095 | 4.9326 | 0.20890 | 184.8 | 132 | 1366.5 | 2 | 0.00780 | 0.055 | 29.5 |
| 3 | 58.5 | 1830 | 16 | 1.098 | 12.304 | 0.27468 | 186.5 | 162 | 1499.7 | 3.7 | 0.00630 | 0.065 | 31 |
| 4 | 117.5 | 1830 | 17 | 1.099 | 24.751 | 0.403480 | 187.2 | 209 | 1623.8 | 5.5 | 0.00521 | 0.098 | 33 |
| 5 | 176 | 1830 | 18 | 1.104 | 37.224 | 0.52963 | 190.6 | 269 | 1892.9 | 17 | 0.01232 | 0.13 | 35.8 |
| 6 | 235 | 1830 | 17 | 1.099 | 49.511 | 0.69394 | 181.4 | 336 | 2608.0 | 165.6 | 0.30243 | 0.18 | 37.9 |
| 7 | 5 | 700 | 18 | 1.102 | 0.4040 | 0.12480 | 80.80 | 190 | 1759.4 | 2 | 0.04908 | 0.02 | 29.8 |
| 8 | 194 | 2800 | 16 | 1.099 | 62.495 | 0.71288 | 251.3 | 391 | 5002.0 | 177 | 0.15093 | 0.2 | 43 |
| 9 | 145.5 | 2800 | 18 | 1.103 | 47.059 | 0.57465 | 243.7 | 343 | 4483.0 | 133 | 0.02704 | 0.16 | 40.4 |
| 10 | 97 | 2800 | 19 | 1.104 | 31.414 | 0.45785 | 239.2 | 284 | 3946.1 | 88.5 | 0.02385 | 0.14 | 38.3 |
| 11 | 48.5 | 2800 | 21 | 1.110 | 15.783 | 0.32025 | 244.6 | 223 | 3389.8 | 28 | 0.01363 | 0.11 | 37.5 |
| 12 | 19.5 | 2800 | 21 | 1.111 | 6.3530 | 0.24926 | 246.5 | 189 | 3069.3 | 19.4 | 0.02199 | 0.081 | 35.2 |
| 13 | 5 | 700 | 21 | 1.110 | 0.4069 | 0.12538 | 74.40 | 103 | 1628.6 | 3 | 0.05478 | 0.013 | 25.6 |

Table 5: Waste gate opening range No. 7

| Mode No. | Torque (N.m) | Speed (rpm) | $T_c$ °C | $C_f$ | $P_{b,s}$ (kW) | Eq. ratio | $\dot{m}_{air}$ (kg/h) | $T_{exhaust}$ °C | $P_{exhaust}$ (Pa) | $\rho_{soot}$ (mg/m$^3$) | $S_{soot}$ (g/kWh) | $P_{inlet\ manifold}$ (bar) | $T_{inlet\ manifold}$ °C |
|---|---|---|---|---|---|---|---|---|---|---|---|---|---|
| 1 | 5 | 700 | 11 | 1.085 | 0.3976 | 0.12131 | 84.9 | 85 | 1244.8 | 2.9 | 0.05915 | 0.0037 | 17 |
| 2 | 23.5 | 1830 | 13 | 1.09 | 4.9094 | 0.20556 | 197.7 | 131 | 1286.1 | 0.35 | 0.00147 | 0.070 | 27.5 |
| 3 | 58.5 | 1830 | 14 | 1.092 | 12.238 | 0.25520 | 199 | 157 | 1422.7 | 3.9 | 0.00703 | 0.10 | 29.5 |
| 4 | 117.5 | 1830 | 14 | 1.093 | 24.62 | 0.36653 | 205 | 204 | 1502.6 | 5.4 | 0.00556 | 0.15 | 34 |
| 5 | 176 | 1830 | 16 | 1.096 | 36.982 | 0.46323 | 215 | 247 | 1761.9 | 12.6 | 0.00991 | 0.21 | 39 |
| 6 | 235 | 1830 | 18 | 1.104 | 49.713 | 0.58299 | 222 | 294 | 2462.6 | 69 | 0.14225 | 0.26 | 44.5 |
| 7 | 5 | 700 | 16 | 1.098 | 0.40238 | 0.11893 | 78.8 | 123 | 1448.7 | 2.9 | 0.05983 | 0.019 | 26.8 |
| 8 | 194 | 2800 | 16 | 1.099 | 62.503 | 0.57751 | 320.89 | 349 | 4852.9 | 162.4 | 0.16438 | 0.35 | 53.9 |
| 9 | 145.5 | 2800 | 19 | 1.105 | 47.132 | 0.42999 | 319.1 | 296 | 4354.8 | 147.6 | 0.03591 | 0.3 | 50.1 |
| 10 | 97 | 2800 | 20 | 1.109 | 31.532 | 0.33132 | 317.8 | 256 | 3821.7 | 100.9 | 0.03391 | 0.25 | 48.5 |
| 11 | 48.5 | 2800 | 21 | 1.11 | 15.784 | 0.25976 | 297 | 199 | 3271.4 | 37.8 | 0.02118 | 0.19 | 43.8 |
| 12 | 19.5 | 2800 | 20 | 1.108 | 6.337 | 0.21728 | 283.2 | 172 | 2860.2 | 25 | 0.03143 | 0.17 | 40.8 |
| 13 | 5 | 700 | 21 | 1.11 | 0.4067 | 0.11360 | 83.6 | 111 | 1570.5 | 3 | 0.06292 | 0.019 | 29 |

**The neural-network model**

A neural network is a general mathematical computing paradigm that models the operations of biological neural systems. The nonlinear nature of neural networks, the ability of neural networks to learn from their environments in supervised as well as unsupervised ways, the universal approximation property of neural networks make them highly suited for solving complex problems[13].

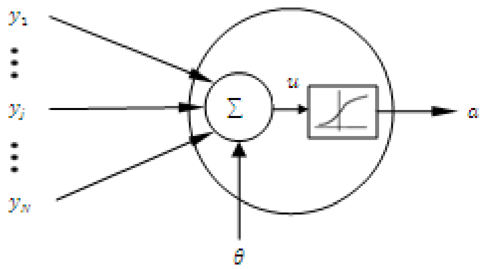


Fig.2. McCulloch and Pitts' neuron model

Neural networks consist of neurons. As shown in Fig.2, each neuron consists of two parts: the net function and the activation inputs $\{y_j; 1 \le j \le N\}$ are combined inside the neuron.

In this figure, a weighted linear combination is adopted:

$$u = \sum_{j=1}^{N} w_j\, y_j + \theta \qquad (10)$$

$\{w_j; 1 \le j \le N\}$ are parameters known as synaptic weights. The quantity θ is called the bias (or threshold) and is used to model the threshold. In the literature, other types of network input combination methods have been proposed [13-14].

The output of the neuron, denoted by $a$ in this figure, is related to the network input $u$ via a linear or nonlinear transformation called the activation function:

$$a = f(u) \qquad (11)$$

In various neural network models, different activation functions have been proposed. In this study sigmoid and pure-line functions are used but you can use any other common used activation functions in modeling process [13-14].

A multilayer perceptron (MLP) neural network model consists of a feed-forward, layered network of McCulloch and Pitts' neurons. Each neuron in an MLP has a nonlinear activation function that is often continuously differentiable. One of the most frequently used activation functions for MLP includes the sigmoid function. A typical MLP configuration is depicted in Fig.3. Each circle represents an individual neuron. These neurons are organized in layers, labeled as the hidden layer #1, hidden layer #2, and the output layer in this figure. While the inputs at the bottom are also labeled as the input layer, there is usually no neuron model implemented in that layer. The name hidden layer refers to the fact that the output of these neurons will be fed into upper layer neurons and, therefore, is hidden from the user who only observes the output of neurons at the output layer. Fig.3 illustrates a popular configuration of MLP where interconnections are provided only between neurons of successive layers in the network [13].

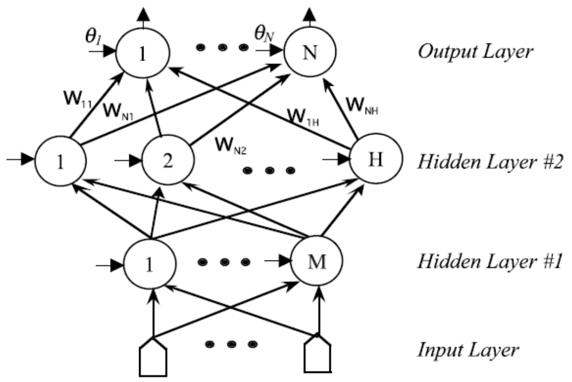


Fig.3. A three-layer multilayer perceptron configuration

An important step when accommodating a neural network is the training. For training an input is introduced to the network with its especial output. The neural network initially chooses the weight and bias values randomly. These values will be updated in each iteration to produce the desired outputs. The weights, after training, contain meaningful information, whereas before training, they are random and have no meaning. When a satisfactory level of performance is reached, the training stops, and the network uses these weights to make decisions.

In this study, the learning algorithm called the back-propagation was applied for the feed-forward network. Backpropagation was created by generalizing the Widrow-Hoff learning rule to multiple-layer networks and nonlinear differentiable transfer functions. Input vectors and the corresponding target vectors are used to train a network until it can approximate a function, associate input vectors with specific output vectors, or classify input vectors in an appropriate way as defined by user. Networks with biases, a sigmoid layer, and a linear output layer are capable of approximating any function with a finite number of discontinuities [15].

As we can see in Fig.4 the ANN model in this study has one hidden layer which has 25 neurons. The inputs for the ANN are inlet manifold pressure, inlet manifold temperature, mass flow rate of inlet air, fuel consumption, torque and engine speed. The output is density of soot in the exhaust manifold. Levenberg–Marquardt (LM) algorithm has been used for training the network. For activation function we used pure-line and logistic sigmoid (logsig). Inputs and outputs of the network are normalized to have values between -1 and 1. This leads to easier training.

The ANN was trained and tested by means of MATLAB software on a PC. For training the neural network six ranges of pressures were used. Seventh range of pressure was kept for testing the accuracy of the trained network. Root mean squared-error (RMSE), fraction of variance ($R^2$) and mean absolute percentage error (MAPE) are defined as follows:

$$RMSE = \sqrt{\frac{1}{N}\sum_{i=1}^{N}(a_i - p_i)^2} \quad (12)$$

$$MAPE(\%) = \frac{1}{N}\sum_{i=1}^{N}\left|100\frac{(a_i - p_i)}{a_i}\right| \quad (13)$$

$$R^2 = 1 - \left(\frac{\sum_{i=1}^{N}(a_i - p_i)^2}{\sum_{i=1}^{N}(a_i)^2}\right) \quad (14)$$

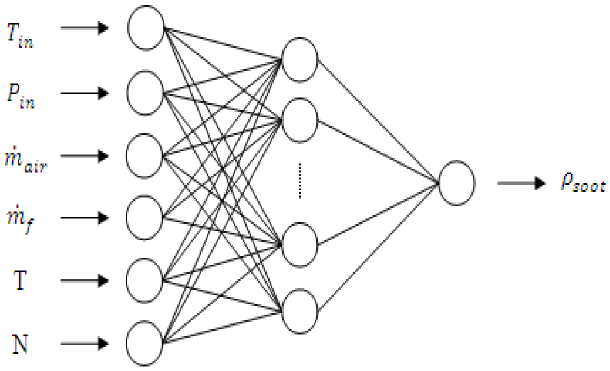


Fig.4. ANN architecture with 25 neurons in a single hidden-layer

## Results and discussion

The ANN predictions for the density of soot emission of the DI diesel engine as a function of the experimental ones are shown in Fig.5. The accuracy of the ANN predictions was evaluated with the help of a straight line indicating the perfect prediction. Also the comparison between actual values and predicted values are shown in Fig.6 and Fig.7. Because the range of soot density is [2-200]$\left(\frac{mg}{m^3}\right)$ we separated high density modes and low density modes in two different charts.

Root mean squared-error (RMSE), fraction of variance ($R^2$) and mean absolute percentage error (MAPE) were found to be 3.4$\left(\frac{mg}{m^3}\right)$, 0.998 and 8.1%respectively. These figures and the magnitude of errors show that the ANN predicts the density of soot emission quite well. It is clear that the performance of the ANN would have been even better if a higher number of test runs had been performed to provide a larger amount of experimental data for the network training.

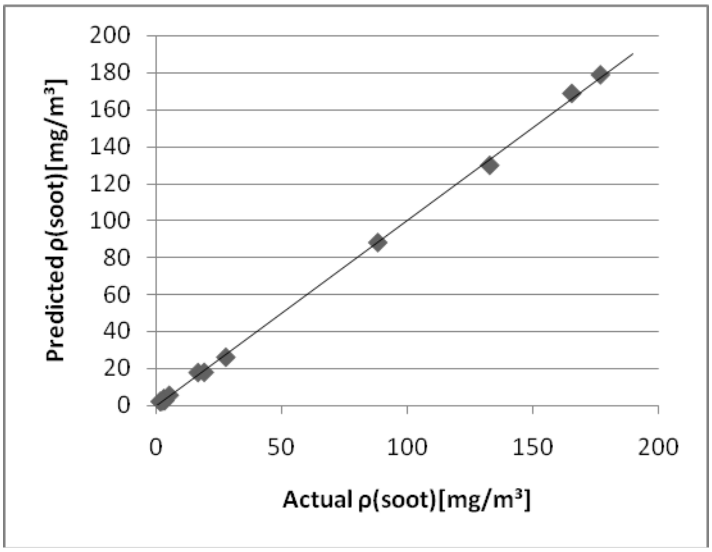


Fig.5. Comparison of actual and ANN approach values for density of soot emission training data

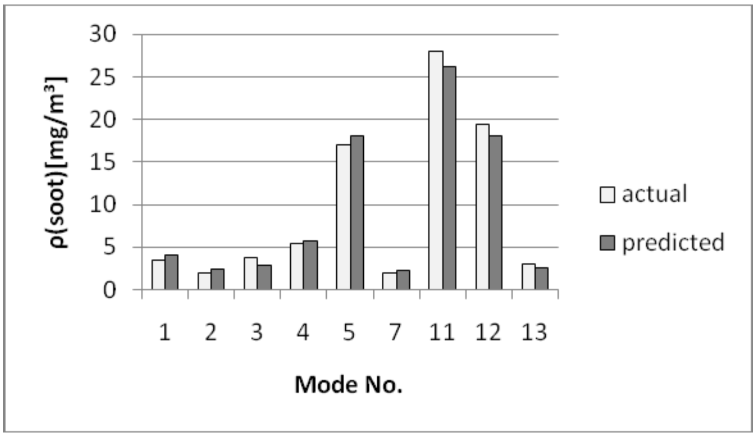


Fig.6. Comparison of actual and ANN approach values for density of soot emission test data(low and average density modes)

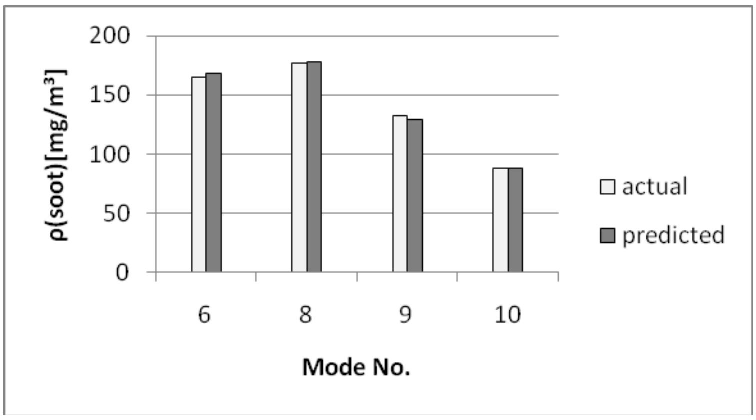


Fig.7. Comparison of actual and ANN approach values for density of soot emission test data(high density modes)

**Conclusion**

This paper wants to show the possibility of using artificial neural networks for predicting the density of soot emission of a turbo-charged DI diesel engine in different opening ranges of waste gate under the ECE-R49, 13 mode standard test. Root mean squared-error (RMSE), fraction of variance ($R^2$) and mean absolute percentage error (MAPE) were found to be $3.4\left(\frac{mg}{m^3}\right)$, 0.998 and 8.1% respectively. These results show that, in most cases, the network produces values close enough to the experimental data. So this model can be used as an alternative for the tested engine and it can help us to study the amount of soot emission. Therefore in other applications like this that we have enough experimental data we can use this approach to reduce the experimental testing and consequently save time and money.

**Nomenclature**

| | |
|---|---|
| $A_0$ | Orifice area |
| $C_D$ | Discharge coefficient |
| $C_f$ | Power correction factor |
| $\dot{m}_a$ | Air mass flow rate |
| $\dot{m}_f$ | Fuel mass flow rate |
| $\dot{m}_{soot}$ | Soot mass flow rate |
| $N$ | Engine speed |
| $P_b$ | Engine brake power |
| $P_m$ | Measured ambient-air absolute pressure |
| $P_{v,m}$ | Measured ambient-water vapor partial pressure |
| $P_{s,d}$ | Standard dry-air absolute pressure |
| $P_e$ | Exhaust pressure |
| $P_i$ | Inlet manifold pressure |
| $\dot{Q}_e$ | Volumetric flow rate of exhaust gas |
| $S_{soot}$ | Specific soot emission |
| $T$ | Engine torque |
| $T_e$ | Exhaust temperature |
| $T_m$ | Measured ambient –air temperature |
| $T_s$ | Standard ambient –air temperature |
| $t_f$ | Required time for consumption of 50 cc of fuel |
| $w_f$ | Weighting factor |
| $\Delta h_{orific}$ | Difference in elevation of orifice |
| $\rho_{soot}$ | Exhaust soot density |
| $\rho_{air}$ | Intake air density |
| $\rho_e$ | Exhaust gas density |
| $\rho_l$ | Manometr liquid density |
| $t_f$ | Required time for consumption of 50 cc of fuel |
| EVO | Exhaust Valve Opening |
| O.R.W.G | Opening range of waste gate |
| W.G. | Waste-gate |
| ANN | Artificial neural-network |
| LM | Levenberg–Marquardt |
| RMSE | Root mean squared-error |
| $R^2$ | Fraction of variance |
| MAPE | mean absolute percentage error |
| MLP | Multilayer Perceptron |
| $\Phi$ | Equivalence ratio |

**References**

[1]- George Sam, and Balla Santhosh, and Gautam Vishaal, and Gautam Mridul, "Effect of diesel soot on lubricant oil viscosity," USA. Tribology International, Vol. 40, pp. 809-818, 2007.

[2]- Tree, D. R., and Svensson, K. I., "Soot processes in compression ignition engines," Progress in Energy and Combustion Science, Vol. 33, pp. 272-309, 2007.

[3]- Pickett, L. M., and Siebers, D. L., "Soot in diesel fuel jets: effect of ambient temperature, ambient density, and injection pressure," Combustion and Flame, Vol. 138, pp. 114-135, 2003.

[4]- Deng Yuanwang, and Zhu Meilin, and Xiang Dong, and Cheng Xiaobei, "An analysis for effect of cetane number on exhaust emissions from engine with the neural network," Fuel, Vol. 81, pp. 1963–1970, 2002.

[5]- Durana, A., and Lapuertab, M., and Rodriguez-Fernandezb, J., "Neural networks estimation of diesel particulate matter composition from transesterified waste oils blends," Fuel, Vol. 84, pp. 2080–2085, 2005.

[6]- Mustafa Canakci, and Ahmet Erdil, and Erol Arcaklioglu, "Performance and exhaust emissions of a

biodiesel engine," Applied Energy, Vol. 83, pp. 594–605, 2006.
[7]- Veli Celik, and Erol Arcaklioglu, "Performance maps of a diesel engine," Applied Energy, Vol. 81, pp. 247–259, 2005.
[8]- Cenk Sayin, and Metin Ertunc, H., and Murat Hosoz, and Ibrahim Kilicaslan, and Mustafa Canakci, "Performance and exhaust emissions of a gasoline engine using artificial neural network," Applied Thermal Engineering, Vol. 27, pp. 46–54, 2007.
[9]- Mustafa Golcu, and Yakup Sekmen, and Perihan Erduranlı, and Sahir Salman, M., "Artificial neural-network based modeling of variable valve-timing in a spark-ignition engine," Applied Energy, Vol. 81, pp. 187–197, 2005.
[10]- Youhong Yu, and Lingen Chen, and Fengrui Sun, and Chih Wu, "Neural-network based analysis and prediction of a compressor's characteristic performance map," Applied Energy, Vol. 84, pp. 48–55, 2007.
[11]- Ghazikhani, M., and Davarpanah, M., and Moosavi Shayegh, S. A., "An experimental study on the effects of different opening ranges of waste-gate on the exhaust soot emission of a turbo-charged DI diesel engine," Energy Conversion and Management, Vol. 49, pp. 2563–2569, 2008.
[12]- http://www.Dieselnet.com/standards/eu/hd.htm
[13]- Yu Hen Hu, and Jenq-Neng Hwang, *Handbook of neural network signal processing,* CRC Press. 2001
[14]- Beale, R., and Jackson, T., *Neural Computing: An Introduction,* Institute of Physics Publishing. 1998.
[15]- Matlab Version 6.5 Online Manual.